JOURNAL OF MATERIALS SCIENCE: MATERIALS IN MEDICINE **16** (2005) 967–975

Hot compaction of poly(methyl methacrylate) composites based on fiber shrinkage results

D. D. WRIGHT-CHARLESWORTH[1,*], E. P. LAUTENSCHLAGER[2], J. L. GILBERT[3]
[1]*Department of Biomedical Engineering, Michigan Technological University, 1400 Townsend Dr., Houghton, MI 49931*
[2]*Division of Orthopaedics/Biomaterials, Northwestern University, 320 E. Superior Ave., Chicago, IL 60611*
[3]*Department of Bioengineering and Neuroscience, Syracuse University, Link Hall, Syracuse NY 13244*

Uniaxial self-reinforced composite poly(methyl methacrylate) (SRC-PMMA) is being investigated as a pre-coat material for the femoral component of total hip replacements. Hot compaction of self-reinforced composites is largely an empirical process which varies the processing parameters of time, temperature and pressure until the desired properties are obtained. Previous work has shown that PMMA fibers have unique thermal relaxation properties dependent upon the retained molecular orientation in them. This work processed composites at times and temperatures that span the relaxation process for a single fiber. It was found that molecular orientation, as measured by birefringence, was lost in composites processed at times greater than relaxation times for single fibers. Flexural properties were also found to vary with processing conditions, with the highest values of 165 $\pm$ 15 MPa and 168 $\pm$ 3 MPa found at high and low processing times, respectively. These are significantly stronger than unreinforced PMMA which has a flexural strength of 127 $\pm$ 14 MPa. It is hypothesized that diffusion between fibers occurs much more quickly than the loss of molecular orientation and it was seen that SRC-PMMA processing conditions can be predicted from the relaxation times and temperatures from single fibers.

1. Introduction

Self-reinforced composites (SRCs) can be fabricated from any thermoplastic fibrous material. Fibers are heated and press together under pressure to form a matrix directly from the fibers as the outer surfaces bond together. Ward *et al.* have used this method with great success with polyethyelene (PE) [1–9] poly(ethylene terephthalate) [10], and polypropylene fibers [11]. Törmälä and colleagues have performed the most extensive studies with poly(lactic acid) (PLA) and poly(glycolic acid) (PGA) SRCs [12–35]. Degradable SRCs from PLA and PGA are being used as fracture fixation pins and screws (Linvatec).

SRCs have also been fabricated from poly(methyl methacrylate) (PMMA) [36, 37]. SRC-PMMA has shown improved properties over bone cement, and is being investigated as a pre-coat for total hip replacements. Results for SRC-PMMA show improved mechanical properties, including bending strength [37, 38], fracture toughness [37–39], fatigue [38], tensile strength [38] and wear [40] Since the fiber and matrix of the composite have the same chemistry, there are significant advantages in using SRCs for medical applications. Traditional composite laminate materials are prone to delamination *in vivo* [41]. Water is able to infiltrate the laminates and reduces the stiffness of the materials too rapidly to be used in implantable devices. In a SRC, the matrix and fiber have the ability to form a stronger bond due to the similarity in chemistry between the components. Additionally, biocompatibility is a major concern with new materials. The FDA approval process is lengthy and cost prohibitive, leading to reluctance from companies to adopt new materials. If the composites are fabricated from one material with a proven biocompatibility, it may be easier to determine their *in vivo* response. PLA and PGA, for example, are both FDA approved materials as neat materials and SRCs. The biocompatibility of these materials is similar in both animal and human use.

Despite the success of these materials and potential benefits for medical devices, processing of SRCs remains an empirical procedure. SRCs are typically processed at a range of times, temperatures and pressures, and the best composite is selected based on a desired material property. Polymer fibers, however, have unique thermal shrinkage properties depending on the amount

*Author to whom all correspondence should be addressed.

of retained molecular orientation [42]. Because the polymer chains are oriented, they shrink when heated. If they are constrained, the shrinkage results in a stress that can be measured as a function of time and temperature. The development of this stress is related to the initial relaxation and untangling of molecules, while the decay of the stress represents the complete disentanglement of the polymer network. During processing of an SRC, it is desired to form a strong bond between the fibers while maintaining molecular orientation. Molecular orientation results in fiber strength, but a strong matrix is also necessary for good mechanical properties in a composite. Hypothetically, if composites are processed in between the time it takes for the shrinkage stress to develop and decay, the resultant material will have a strong matrix and retained fiber orientation.

The goal of this work is to use the thermal shrinkage properties of single fibers to predict processing conditions to optimize flexural properties for SRC-PMMA.

2. Materials and methods

2.1. Fibers

Fibers, nominally 52 μm in diameter, were fabricated using poly(methyl methacrylate) (PMMA, V045, Atohaas) and a method described in detail previously [43]. Briefly, PMMA was ram extruded through a heated die and spun onto a takeup wheel. The difference between this study and previous work [43] was that a die with thirteen 1mm holes was utilized instead of a single hole die to speed fiber production. An extrusion velocity of 0.127 cm/min was used, which is ten times faster than the rate used previously [43] to account for the increase in area at the die exit. A draw velocity of 2594 cm/min was used to maximize the fiber strengths. Tensile and heat relaxation ratio (HRR) properties of these fibers were characterized using previously described methods [43], and are shown in Table I. HRR measures the length of the fiber before and after being heated to well above the glass transition temperature, and measures the relative amount of orientation present in the fiber.

Constrained fiber shrinkage tests characterized the thermal properties of the fibers using a method described in detail previously [42]. A fiber 2.54 cm long was placed in the grips with no pre-tension. A preheated oven was raised to completely surround the fiber, and the force that resulted from the polymer molecules losing their orientation was measured as a function of time and temperature. Fiber shrinkage experiments were performed at a temperature range of $100\,^{\circ}\mathrm{C} \leq T \leq 180\,^{\circ}\mathrm{C}$ with two or three samples at each temperature. Time constants for the rates of development and decay of the stress are plotted versus the inverse of temperature in Fig. 1 and obey an Arrhenius relationship with temperature. Note that low temperatures are on the right hand side of the graph, and short times are toward the top. The time constants for the rise process lie on a line above those for the decay process. The maximum shrinkage stresses was 8.98 ± 0.71 MPa at all temperatures.

TABLE I HRR properties of fibers fabricated for composite production

Property	Value
Fiber diameter (μm)	51.99 ± 6.84 ($n = 16$)
HRR	18.59 ± 1.88 ($n = 6$)
True UTS (MPa)	172.8 ± 33.7 ($n = 5$)
Modulus (GPa)	3.72 ± 0.67 ($n = 5$)
True strain at failure (%)	12.86 ± 3.36 ($n = 5$)

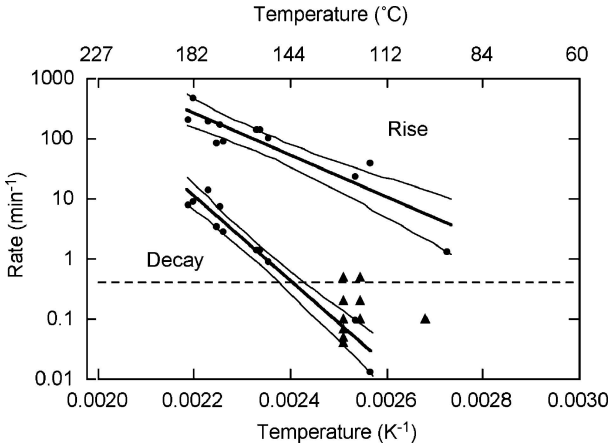

Figure 1 Arrhenius curves for rise and decay of relaxation stresses of single fibers used in composite processing. The rise process lies above the decay process. The fibers were fabricated using a 13 hole die at a temperature of 219 °C and draw velocity of 2594 cm/min. The small dots represent the fiber shrinkage measurements, and the triangles represent the processing conditions for composites. The dashed line represents the fastest processing rate attainable with the hot compaction press used.

2.2. Composite fabrication

Unidirectional SRC-PMMA composites were fabricated using the fibers described above and a channel mold. The channel dimensions were 12.7 × 254 mm. For each composite, 12 g of fiber were placed in the channel, and a bar was placed on top. Fibers were aligned along the long axis of the channel. The mold assembly was then placed in a pre-heated lamination press (Wabash MPI, Wabash IN). In hot compaction processing, the independent processing variables are pressure, time and temperature. The force applied during processing ranged from 5.3 to 23.1 kN (1.65 to 7.17 MPa of pressure when divided by the area of the channel). During processing, the force decreased as the

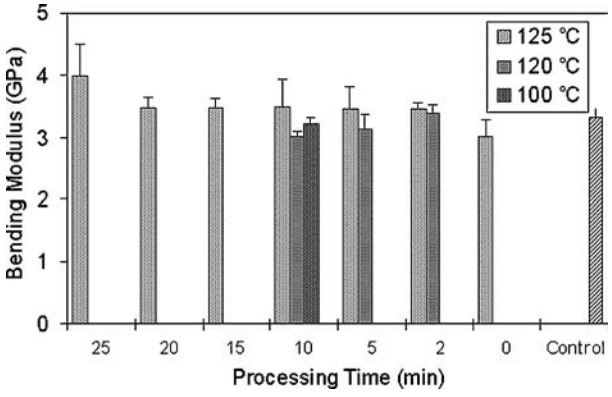

Figure 2 Bending modulus for composites and plexiglas control. Bars represent the mean ± standard deviation. Each processing temperature is represented by a different shaded bar, as shown in the legend.

TABLE II Summary of processing conditions for composites

Label	Processing temperature (°C)	Processing time (min)
V1	125	25
V2	125	20
V3	125	15
V4	125	10
V5	125	5
V6	125	2
V7	125	0
V8	120	2
V9	120	5
V10	120	10
V11	100	10

polymer consolidated, deformed into polygonal shapes and flowed out of the mold and around the press bar. When the force reached 5.3 kN, it would automatically increase to 23.1 kN. For samples processed longer than 10 min, the force was reapplied twice. For samples processed between 2 to 5 min, force was reapplied once.

The temperature of the press decreased once the mold was placed in it and regained the set temperature after approximately 2.5 min. Once cooling began, the temperature of the platens dropped to 90 °C in approximately 1.5 min. The time reported for processing conditions was from when the mold regained the set temperature to the beginning of the cooling cycle.

Processing times and temperatures were chosen based on the constrained fiber shrinkage curve in Fig. 1, where each processing condition is shown as a triangle. The shortest processing time available was the time necessary to regain the set temperature, or 2.5 min, which corresponded to a rate of 0.4 min^{-1}. This provided an upper limit on the processing capabilities of this press with this mold. This is shown as a dashed line in Fig. 1. Processing times were chosen at three temperatures to span the decay time constant line. Since the decay rate represents the rate needed for 63% relaxation of a polymer fiber, processing times chosen above the line should have retained molecular orientation, while times below the line should result in composites with no retained molecular orientation. The processing conditions are summarized in Table II along with labels that will be used to refer to the composites.

2.3. Bending

A three point bend test of the composite was used to determine the maximum bending stress, bending modulus and strain to failure of the material. Bending specimens were sectioned from the composite bars using an Isomet low speed saw (Model 11-1180, Bueler, Lake Bluff IL) lubricated by water. The samples had a nominal length of 42 mm and width of 6.5 mm. The thickness of the samples varied from 1.13 to 2.09 mm, with an average of 1.69 mm. One sample group (V7) had a thickness of 2.5 mm. This group was not processed long enough to accomplish complete bonding between the fibers, as evidenced by fibers protruding from the sample, which accounts for its extreme thickness. A minimum of four samples were tested in each of the experimental groups. Control specimens ($n = 6$) were fabricated from a sheet of commercially available acrylic (Plexiglas®). The average dimensions of the control samples were 45.13 × 6.21 × 1.76 mm. All specimens were polished to a grit of 600 using a Handimet grinder (Bueler, Lake Bluff IL) to ensure that surface flaws minimally affected the result of the test.

Three-point bending tests were conducted on a mechanical testing system (Instron Model #1114, Canton MA). The span of the supports was 20 mm, resulting in a span:thickness ratio ranging from 9.6:1 to 17.7:1. The ASTM standard calls for span:thickness ratios ranging from 14:1 to 20:1 [44]. Previous work [45] has shown that decreasing the span:thickness ratio results in an increase in the shear stress at the loading point. It was also shown that for a span:thickness ratio of 9.36:1, the error induced by the increase in shear stress was 0.14%. Therefore, for the samples in this study, the effects of decreasing the span:thickness ratio can be assumed to be negligible. The crosshead was lowered at a rate of 25.4 mm/min. This rate is significantly faster than the rate suggested by the ASTM standard [44], approximately 0.4 ± 0.2 mm/min. The rate of 25.4 mm/min was chosen based on preliminary work to ensure that the samples were failing before the loading nose struck the supports. At a lower rate of testing (2.54 mm/min), the experimental samples were not failing, but simply yielding. A more complete discussion of the rate used and its effects on testing is included in the discussion section. The slope (M, N/mm) of the initial straight line portion of the load-deflection curve was measured as well as the maximum load (P, N) and deflection at failure (D, mm). The maximum stress (σ, MPa) was calculated by [44]

$$\sigma = \frac{3PL}{2db^2}$$

where L is the span length (20 mm), b is the width of the sample (mm) and d is the thickness of the sample (mm). The bending modulus (E_b, MPa) was calculated according to [44]

$$E_b = \frac{L^3M}{4bd^3}$$

where all the quantities have been previously defined. The strain at failure (r, %) was calculated by [44]

$$r = \frac{6Dd}{L^2}$$

where all of the quantities have been previously defined.

Statistical analysis was performed using Statistica. One-way and two-way Analysis of Variance (ANOVA) was used, as appropriate, with a Newman-Keuls *post-hoc* test to determine differences between groups. Independent variables were processing conditions (time, temperature, or both) and dependent variables were the measured mechanical properties. A $p \leq .05$ was considered statistically significant.

2.4. Microscopy

Representative composite and control specimens were imaged using Scanning Electron Microscopy (SEM, Cambridge Instruments S120). Samples were mounted in acrylic so that the fracture surface was exposed, and subsequently coated with gold.

3. Results

3.1. Composite fabrication

Composites fabricated at the processing conditions listed in Table II were viewed under polarized light. Bright colors indicate that there is residual orientation in the composite material. Birefringent colors are seen at processing times at or below 5 min for composites fabricated at 125 or 120 °C (groups V5, V6, V7, V9, V10, V11).

3.2. Bending

Figs. 2 and 3 show the results for the bending modulus and strength of composites as a function of processing time. Bending strength is the highest at low and high processing times. At 120 °C, high strengths were noted at the low processing time, but samples were not fabricated at high processing times. Table III lists the results for strain to failure. For samples that did not fail, the test was ended at a deflection of 8 mm. At this point, the samples were bent at a 90° angle, and the loading nose began to hit the support. A strain at the end of the test is calculated for these samples. This does not represent the ultimate strain to failure, but it does provide a lower limit on the strain to failure.

One-way ANOVAs with *post hoc* Newman-Keuls tests were used to determine if processing temperature or time had a statistical effect on the bending strength or modulus. At 125 °C, the highest strengths were found at processing times of 2, 20 and 25 min (Table IV). In general, the modulus was highest at a processing time of 25 min, and the lowest at 0 min (Table V). At a constant processing time of 10 min, the highest strengths were found at the lowest processing temperature, 100 °C. The strengths at 120 and 125 °C were statistically identical. Temperature had no statistically significant effect with regard to bending modulus at processing times of 10 min.

A two-way ANOVA was used to determine the interactive effects of processing time and temperature on bending strength and modulus. Composites processed at 120 and 125 °C at processing times of 2, 5 and 10 min were compared. There were no statistical differences between any of the composites for the modulus of elasticity. The interactive effects are listed in Table VI for bending strength. There was no difference between samples processed at the same time and different temperatures. Decreasing the processing time while keeping the processing temperature in the range of 120–125 °C increased the bending strength of the composites while having no effect on the modulus.

Strain to failure results for the composites and control sample were pooled together to determine statistical differences for the samples that broke. Samples that broke showed similar fracture mechanisms in a visual, and later SEM, examination of the fracture surface. As shown in Table III, samples that did not break had higher strains at the end of the test than the samples that fractured. However, it is not possible to determine statistical differences between these groups because they were

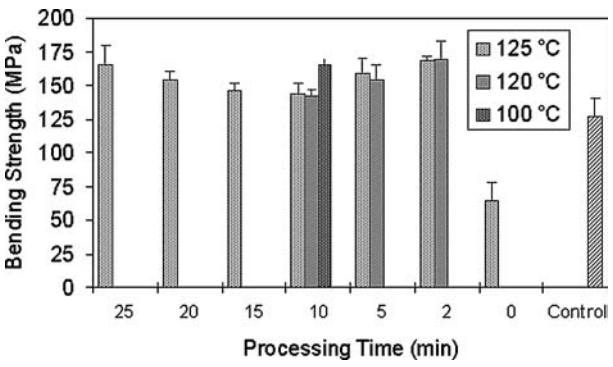

Figure 3 Bending strength for composites and plexiglas control. Bars represent the mean ± standard deviation. Each processing temperature is represented by a different shaded bar, as shown in the legend.

TABLE III Strain to failure for SRC-PMMA bending specimens

Sample label	Strain to failure (%)	Strain at end of test (%)
V1	7.0 ± 0.5 ($n = 3$)	13.3 ($n = 1$)
V2	7.5 ($n = 1$)	16.8 ± 0.2 ($n = 3$)
V3	8.2 ($n = 1$)	14.0 ± 0.4 ($n = 4$)
V4	6.6 ($n = 1$)	13.8 ± 0.3 ($n = 5$)
V5	14.5 ($n = 1$)	19.3 ± 0.8 ($n = 5$)
V6	N/A ($n = 0$)	22.0 ± 0.5 ($n = 5$)
V7	N/A ($n = 0$)	30.7 ± 1.6 ($n = 6$)
V8	N/A ($n = 0$)	23.7 ± 1.3 ($n = 5$)
V9	N/A ($n = 0$)	20.3 ± 1.5 ($n = 6$)
V10	8.4 ± 2.6 ($n = 2$)	18.8 ± 0.6 ($n = 4$)
V11	N/A ($n = 0$)	22.2 ± 0.8 ($n = 6$)
Control	4.4 ± 1.2 ($n = 6$)	N/A ($n = 0$)

TABLE IV *Post hoc* results for comparing the bending strength of composites fabricated at 125 °C as a function of processing time. A $p <$ .05 was considered significant, and is marked by a "+"

Time	0	2	5	10	15	20	25
Mean σ	64.6	168.0	158.9	144.2	146.2	154.1	164.9
0		+	+	+	+	+	+
2	+			+	+		
5	+						
10	+	+					+
15	+	+					+
20	+						
25	+			+	+		

TABLE V *Post hoc* results for comparing the bending modulus of composites fabricated at 125 °C as a function of processing time. A $p <$ .05 was considered significant, and is marked by a "+"

Time	0	2	5	10	15	20	25
Mean E	3.00	3.44	3.45	3.50	3.47	3.48	3.99
0		+					+
2	+						
5							
10							+
15							
20							+
25	+			+		+	

TABLE VI *Post hoc* interaction results for a two-way ANOVA for composites. The two independent variables are the processing time and temperature, and the dependent variable is the bending strength

Proc. time	2	2	5	5	10	10
Proc. temp.	120	125	120	125	120	125
Mean	169.6	168.0	153.7	158.9	142.3	144.2
2 120			+		+	+
2 125			+		+	+
5 120	+	+				
5 125					+	+
10 120	+	+		+		
10 125	+	+		+		

not able to be tested to failure. A t-test showed that the composites broke at a statistically higher strain than the control specimens ($p < .0005$). Thus, even without including the results from the specimens that did not break, SRC-PMMA has a higher strain to failure than the control samples.

3.3. Fracture mechanisms

3.3.1. Visual observations

Samples were visually examined and photographed before being gold coated and examined by SEM. Several different fracture mechanisms were noted dependent upon the processing conditions of the composites. The control specimens all fractured in a clean fashion, with flat fracture surfaces. One sample had a curved fracture surface, with a lip protruding on the compressive side of failure. The fracture surface had a flat appearance, with a thumbnail shaped fracture initiation point and subsequent scalloping radiating out from the apparent fracture point.

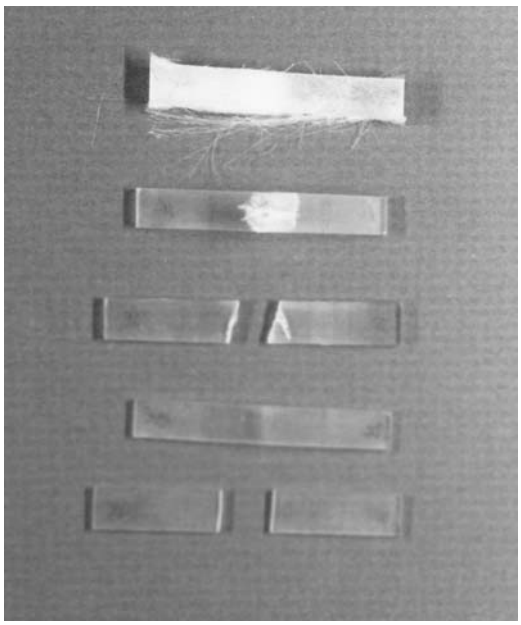

Figure 4 Photograph of bending specimens after testing. Composites were fabricated at a processing temperature of 125 °C. Processing times are 0, 2, 5, 15 and 25 min from top to bottom.

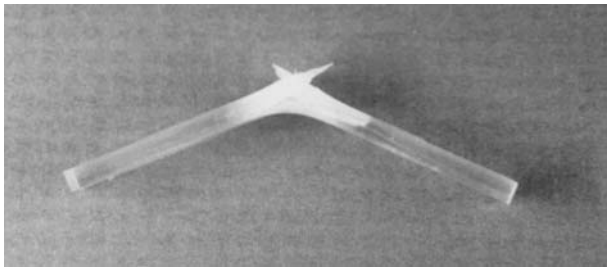

Figure 5 Photograph of bending specimen after testing. Composite was fabricated at a processing temperature of 125 °C and processing time of 2 min.

Fig. 4 shows composites fabricated at 125 °C and a range of times. In general, decreasing the processing time or temperature led to extensive fiber/matrix damage. At intermediate times, there was very little breakage, and most samples simply bent at a 90° angle, and testing had to be discontinued. For example, composites processed at 2 min and 125 °C had two samples with severe damage as pictured in Fig. 5. At 120 °C and 2 min, the mechanism illustrated in Fig. 5 was seen for all samples. The sample processed for 10 min at 100 °C also showed extensive fiber/matrix damage as shown representatively in Fig. 5. At higher processing times, brittle fracture took place for more of the samples. See Table III for a summary of the number of broken specimens for each composite type.

3.3.2. SEM

SEM verified and expanded upon the previous visual observations. Except where noted, the tensile side of the specimen is on the left hand side of the micrograph, and the fracture proceeds from left to right. In Fig. 6, a control sample is seen. The classical brittle fracture of PMMA is evident, with the sunburst pattern emanating from the fracture initiation site. The flat portion of the acrylic is the initiation site for the fracture, and once brittle fracture occurs, failure continues rapidly through the rest of the sample.

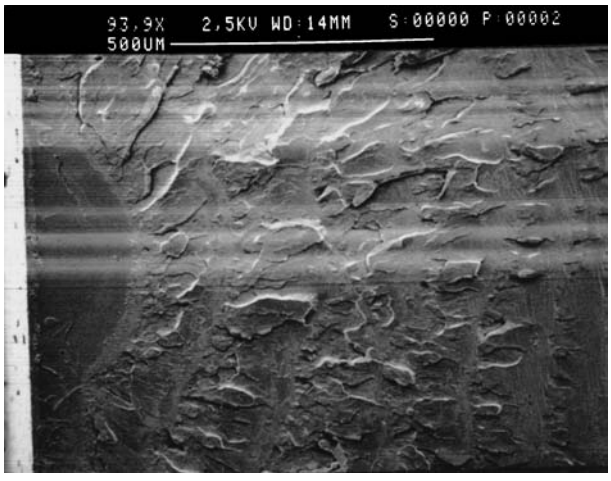

Figure 6 SEM of control sample. The thumbnail shaped flat area with sunburst pattern emanating from it is the site of fracture initiation.

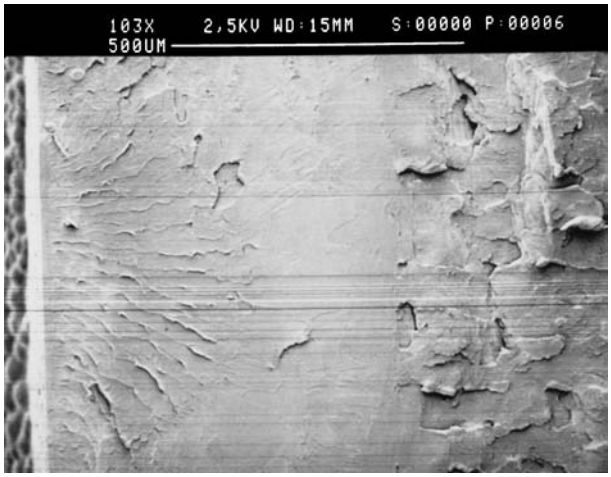

Figure 7 Composite processed for 10 min at 125 °C. A rippled fracture surface is seen at the fracture initiation site, and indentations which are possible pull out locations for fibers are seen.

Figure 9 Composite processed for two minutes at 125 °C. The tensile surface is shown.

Fracture mechanisms for the composites change as a function of processing time and temperature and are markedly different than for the control samples. At 125 °C, a specimen processed for 10 min is shown in Fig. 7. In contrast to Fig. 6, the fracture initiation site is rippled at the tensile surface. For the control sample, the initiation site was perfectly flat. The ripples in the composite specimen indicate that crack propagation is more difficult, and there are indentations in the surface that may be remnants of oriented fibers "pulling out" of the fracture surface. At a higher processing time of 25 min, the surface is similar. At a processing time of 5 min, the one sample that broke exhibited a curved surface, as shown in detail in Fig. 8. The tensile surface for this specimen would be just out of the field of view on the left. At the left hand side of Fig. 8, cracking into the matrix can be seen, and the scalloped surface can be seen in the center. The scalloped surface and angled nature of the surface indicates shear fracture of the composite through the fibers. At the lowest processing time of 2 min, the specimen does not break, but bends. The tensile surface of one of these specimens is shown in Fig. 9. The cracks emanated from the surface in an angled fashion, and the fibrous nature of the sample can be seen in the remnants of matrix and fiber that look like tendrils in the v-shaped fracture.

At 120 °C, the progression of fracture surfaces is similar to that discussed for 125 °C. At 10 min, the surface is similar to that shown in Fig. 7. At two min, the fracture surface is seen in Fig. 10 and can be contrasted with Fig. 9. These samples did not break, and the tensile side of the sample is shown in the figure. At the lower temperature, the fibrous nature of the sample is more clear, and matrix cracking and fiber splitting can be seen. At higher magnification, shown in Fig. 11, this can be seen very clearly. There are tags on the surface that may be remnants of matrix or neighboring fibers. The fibers have a scalloped appearance, indicating that they have been damaged by splitting. At the lower temperatures, bonding between the fibers is not as complete as at the higher temperatures, and damage occurs primarily through matrix cracking and fiber splitting, rather than by shear fracture of the composite as shown in Fig. 9.

At the lowest processing temperature of 100 °C and 10 min, the fracture surface is similar to the sample

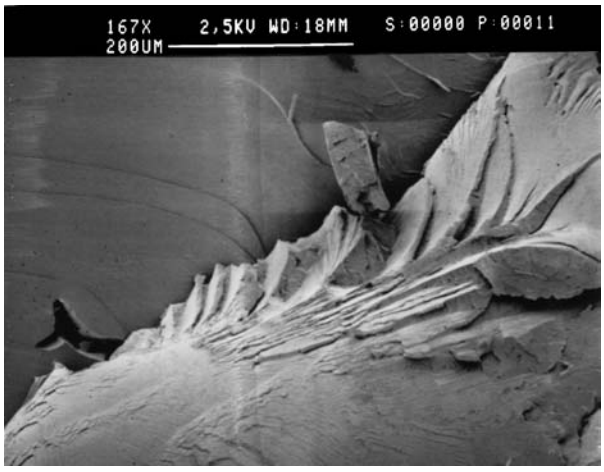

Figure 8 Composite processed for five minutes at 125 °C. A scalloped surface is seen, indicating shear fracture. Cracking into the composite, between the fibers, is seen in the lower left corner.

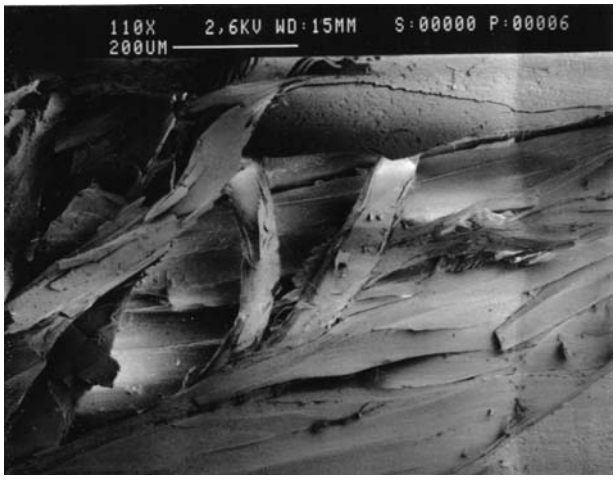

Figure 10 Composite processed for two minutes at 120 °C. The tensile surface is shown. Splitting of fibers, matrix cracking and fiber breakage is shown.

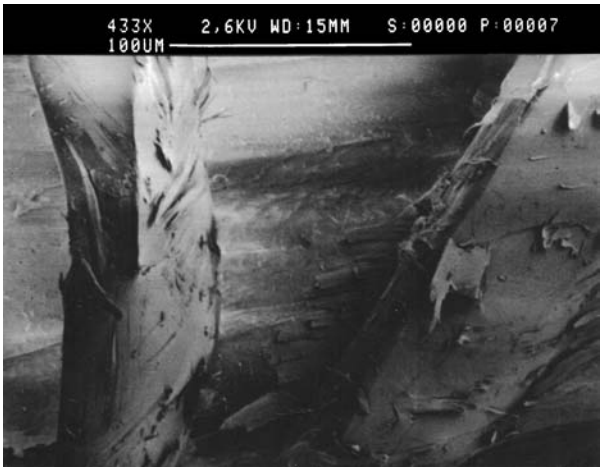

Figure 11 Composite processed for two minutes at 120 °C. A detail of two fibers is shown. Remnants of the matrix can be seen on the fiber surface, and splitting of the fibers can also be seen.

processed at 125 °C for 2 min. The surface is quite fibrous, and failure is occurring with similar mechanisms.

4. Discussion

4.1. Effect of bending rate

Bending tests were conducted at a testing rate of 25.4 cm/min. The ASTM standard calls for a testing rate defined by [44]

$$R = \frac{ZL^2}{6d}$$

where R is the rate of crosshead motion (mm/min), Z is the rate of straining on the tensile surface (defined by ASTM as 0.01 mm mm^{-1} min^{-1}), L is the support span (20 mm) and d is the sample thickness. The sample thickness in these composites ranged from 1.13 to 2.09 mm, with an average of 1.69 mm. At the average thickness, the equation would dictate a testing rate of nominally 0.4 mm/min. This rate can range from 0.2 to 0.6 mm/min, according to the standard.

Initially, tests were conducted at 2.54 mm/min, so that comparisons could be made with previous work, [45] however, the samples were not failing. The load-displacement curves indicated no evidence of failure in the composite, simply yielding until the point where the loading nose began striking the supports of the 3-point bend apparatus. The testing rate was incrementally increased until damage was seen in the specimens. Although some of the samples still did not fracture, a drop in the load was seen earlier for all samples, and damage was seen optically in most samples as small cracks on the tensile side.

The implication of this testing rate is that these composites can be compared to one another and to the control specimen, however, comparison among other polymer specimens tested at different rates is not advisable. At the lower rate of 2.54 mm/min ($L = 25$ mm), for example, the bending strength of the V1 composite was calculated to be 126 ± 2 MPa ($n = 6$, 3 samples broke). At the higher rate of 25.4 mm/min and a span length of 20 mm, the bending strength of the V1 composite was calculated to be 165 ± 15 MPa ($n = 4$, all broke). Polymers are strain rate sensitive materials [46], and increasing the testing rate also increases the bending strength. Fully sintered composites all exhibit better mechanical properties than the control specimens, leading to the conclusion that SRC-PMMA has a higher bending strength than neat PMMA.

4.2. Comparison with previous results

In previous work, longer times and higher temperatures were utilized to process composites. One study [39] investigated the effects of processing time and temperature on the resultant fracture properties of uniaxial SRC-PMMA. Processing times varied between 30–175 min at 128 °C. Processing temperatures ranged from 128–151 °C at 35 min. The pressure was unknown, but very small in this study. At these processing conditions, it was seen that samples had birefringence up to a processing time of 65 min at 128 °C. In this study, birefringence was seen up to processing times of 5 min at 125 °C. These results can be explained when the processing technology is understood. All prior samples [37–39] were processed in an oven and relied on heat transfer from the heated air in the oven through the mold. In this study, heat transfer occurred through pre-heated platens on the press that were maintained at the desired temperature. Heat transfer is much more efficient in the current study, leading to shorter processing times and a more effective fabrication method.

Previous studies with flexural specimens only utilized one processing condition. This condition was empirically chosen based on preliminary work to identify samples that had birefringence and full consolidation of fibers. For comparison, the flexural strength for uniaxial SRC-PMMA was 129.1 ± 14.0 MPa [38], and the strength for woven composites was nominally 75–150 MPa [37], depending on the orientation of the weave. The sample sizes were similar between these studies, however the testing rate in this study is higher than the cited studies. Preliminary work done at the same testing rate as Wright *et al.* [37] indicates that the properties between studies are consistent, even though the processing conditions vary dependent on the equipment used.

4.3. Pressure effects

At this time, it is unknown what effect pressure has on processing SRC-PMMA. Hypothetically, some pressure is required to allow the surfaces of the fibers to be in direct contact with one another, but too much pressure could prevent chain diffusion. In this work, it was seen that bending strength was highest at both low and high processing times at a processing temperature of 120 °C. This could be due to a pressure effect. At the higher times, pressure was reapplied twice, which could lead to more consolidation, or a change in the molecular dynamics of chain motion.

4.4. Competing effects in composite processing

Hot compaction of composites depends on two competing effects: orientation and diffusion. Retained molecular orientation in the polymer fibers strengthens the composite, while diffusion creates the matrix between the fibers. As diffusion increases to strengthen the matrix, orientation decreases in the fiber. Thus, a delicate balance exists between retaining molecular orientation and creating a strong matrix. In previous work [42] it was shown that fibers have unique relaxation properties and differing amounts of retained molecular orientation dependent on the draw velocity and processing temperature. As processing conditions are varied to produce fibers with increasing amounts of retained molecular orientation, the shrinkage stress and rate at which they shrink, increases. It has been hypothesized that processing composites for longer than the decay times will lead to loss of orientation in the fibers, and a subsequent reduction in mechanical properties. In this study, composites have been processed at times above and below the decay times for single fibers. It was not possible to process composites at rates above the rise times for constrained fibers because of the limitations of the hot compaction press and mold. It was noted at extremely short processing times, however, that the samples were not fully incorporated, indicating that the full range of composite processing behavior was explored. The results linking loss of orientation, as measured by the decay times, can now be correlated to composite processing. Previous work has also shown that when composites are viewed under polarized light, they show birefringent colors if orientation is present in the sample [39]. A loss of birefringence is seen as the processing times exceed the decay times, indicating that loss of orientation (as measured by birefringence) is seen at processing times greater than the decay times. These results are confirmed by SEM analysis. In Fig. 7, it is seen that at these high processing times, the fracture mechanisms are more brittle than ductile in nature. As the processing times are decreased, the samples exhibit more ductility, and the samples show shear fracture, matrix cracking and fiber splitting. These failure mechanisms indicate that fiber orientation has been maintained.

The competing effect of diffusion must also be considered. Diffusion of polymer chains between the fibers is required to form a strong matrix in the SRC. If diffusion requires a longer time than the loss of orientation, then fiber processing cannot be linked to the relaxation properties of single fibers. For bulk polymeric materials, diffusion of 100 Å has been determined to provide enough significant entanglements to produce a bond between polymer films being melt pressed [46]. Using a simple Fickian relationship for diffusion and published data for constants, the time required for diffusion of polymer molecules to form the matrix in an SRC can be investigated. Fickian diffusion follows the following equation

$$flux = -D\frac{\Delta C}{\Delta x}$$

where *flux* is the flux of the polymer, D is equal to the diffusion coefficient (cm^2/sec), ΔC is the change in concentration and x is the distance that the polymer must travel. Published values of D have been reported as 10^{-18} to 10^{-14} cm^2/sec for PMMA at temperatures ranging from 120–149 °C [47, 48]. The molecular weights used in these studies are nominally 12,900–980,000 g/mol. The diffusion coefficient is proportional to the inverse of the square of the molecular weight and changes with temperature, however, for a simple approximation, a value of 10^{-16} cm^2/sec will be used.

The concentration of the bulk polymer is the density divided by the weight average molecular weight of the polymer. For the PMMA in this study (M_W = 264,000 g/mol; ρ = 1.18 g/cm^3), this is approximately 4.5×10^{-6} mol/cm^3. Using a value of D as 10^{-16} cm^2/sec, the concentration just calculated, and a distance of 100 Å, the flux of the polymer molecules is 4.5 mol cm^{-2} s^{-1}. To reduce the concentration of polymer molecules at the surface by 10%, 4.5×10^{-8} mol of polymer would need to flow through 1 cm^2. This is most of the polymer that is lying on the surface of the fiber [46], and this diffusion occurs in approximately 0.01 s. The surface area of one fiber is nominally 0.5 cm^2, so this time is roughly equal to the diffusion of 100 Å of polymer between two fibers. Although this is a rough estimate, these times correspond to rates of 6000 min^{-1}, which are well above the rates needed to begin the loss of orientation. Diffusion between polymer fibers will occur almost instantaneously. Most of the time in processing is likely to be used in heating the polymer and mold to the temperature where diffusion occurs.

Based on this analysis, it seems likely that processing of SRC-PMMA can take place at much lower temperatures than previously thought. Although diffusion will slow as the temperature decreases, the diffusion times are orders of magnitude less than τ_{rise}. At a temperature of 120 °C, the time constant for development of the force is 3.7 s. The Arrhenius curves, therefore, represent the upper limit on processing times for SRC-PMMA. Theoretically, composites could be processed at any time and temperature combinations that prevent the loss of orientation in the fibers. Fiber shrinkage curves, therefore, have a profound effect on the design of rational composite processing methods for oriented, amorphous thermoplastics. If the shrinkage properties of the fibers are known, processing times and temperatures can be rationally chosen, which will significantly reduce the trial-and-error currently associated with the fabrication of hot-compacted composites.

5. Conclusions

SRC-PMMA has been fabricated using a hot compaction process and processing conditions based on the fiber shrinkage results from a single fiber. Composites that had retained molecular orientation, as evidenced by birefringent colors under polarized light, were fabricated at temperatures and times that were above the Arrhenius decay time constants for a single fiber. The highest strength composites were fabricated at high and low processing times. At high processing times, the strong matrix and slight residual structural order

provides for strength, while at low processing times, the orientation retained in the fiber leads to high strengths. At intermediate times, enough fiber structure is lost that the fibers do not provide significant strengthening, and the matrix is not fully formed. Previous results [39] showed a maximum in fracture toughness at intermediate processing times, indicating that there are different optimal processing conditions for bending or fracture toughness. The highest strengths were nominally 165 MPa, and represent a significant improvement over the control strength of 135 MPa. Optimal sintering times are more dependent on the time necessary for loss of fiber orientation than the time needed for diffusion to occur.

Acknowledgments

The authors gratefully thank Atohaas for the donation of the V045 acrylic. The American Association of University Women provided a dissertation fellowship (DDW).

References

1. M. J. BONNER, P. J. HINE and I. M. WARD, *Plast., Rubb. Comp. Process. Techn.* **27** (1998) 58.
2. P. J. HINE, I. M. WARD, R. H. OLLEY and D. C. BASSETT, *J. Mater. Sci.* **28** (1993) 316.
3. M. A. KABEEL, D. C. BASSETT, R. H. OLLEY, P. J. HINE and I. M. WARD, *ibid.* **29** (1994) 4694.
4. *Idem.*, *ibid.* **30** (1995) 601.
5. S. S. MORYE, P. J. HINE, R. A. DUCKETT, D. J. CARR and I. M. WARD, *Comp. Part A Appl. Sci. Manuf.* **30** (1999) 649.
6. R. H. OLLEY, D. C. BASSETT, P. J. HINE and I. M. WARD, *J. Mater. Sci.* **28** (1993) 1107.
7. B. TISSINGTON, G. POLLARD and I. M. WARD, *ibid.* **26** (1991) 82.
8. I. M. WARD, *Plast., Rubb. and Comp. Process. Appl.* **19** (1993) 7.
9. D. W. WOODS and I. M. WARD, *Polymer* **29** (1994) 2572.
10. J. RASBURN, P. J. HINE, I. M. WARD, R. H. OLLEY, D. C. BASSETT and M. A. KABEEL, *J. Mater. Sci.* **30** (1995) 615.
11. M. I. ABO EL-MAATY, D. C. BASSETT, R. H. OLLEY, P. J. HINE and I. M. WARD, *ibid.* **31** (1996) 1157.
12. K. P. ANDRIANO, T. POHJONEN and P. TÖRMÄLÄ, *J. Appl. Biomater.* **5** (1994) 133.
13. N. ASHAMMAKHI and P. ROKKANEN, *Biomater* **18** (1997) 3.
14. N. ASHAMMAKHI, H. PELTONIEMI, E. WARIS, R. SUURONEN, W. SERLO, M. KELLOMÄKI, P. TÖRMÄLÄ and T. WARIS, *Plast. Reconstr. Surg.* **108** (2001) 167.
15. E. HIRVENSALO, O. BÖSTMAN, P. TÖRMÄLÄ, S. VAINIONPÄÄ and P. ROKKANEN, *Foot Ankle* **11** (1991) 212.
16. K. JUKKALA-PARTIO, E. K. PARTIO, E. HIRVENSALO and P. ROKKANEN, *Ann. Chir. Gynaecol.* **87** (1998) 44.
17. K. JUKKALA-PARTIO, O. LAITINEN, E. K. PARTIO, J. VASENIUS, S. VAINIONPÄÄ, T. POHJONEN, P. TÖRMÄLÄ and P. ROKKANEN, *J. Orthop. Res.* **15** (1997) 124.
18. T. JUUTILAINEN, E. HIRVENSALO, A. MAJOLA, E. K. PARTIO, H. PÄTIÄLÄ, P. ROKKANEN and J. KINNUNEN, *Ann. Chir. Gynaecol.* **86** (1997) 51.
19. T. JUUTILAINEN, H. PÄTIÄLÄ, M. RUUSKANEN and P. ROKKANEN, *Arch. Orthop. Trauma. Surg.* **116** (1997) 204.
20. M. KELLOMAKI, S. PAASIMAA and P. TÖRMÄLÄ, *Proc. Inst. Mech. Eng. Part H J. Eng. Med.* **214** (2000) 615.
21. K. KOSKIKARE, E. HIRVENSALO, H. PATIALA, P. ROKKANEN, T. POHJONEN, P. TÖRMÄLÄ and G. LOB, *J. Biomed. Mater. Res.* **30** (1996) 417.
22. A. MAJOLA, S. VAINIONPÄÄ, K. VIHTONEN, M. MERO, J. VASENIUS, P. TÖRMÄLÄ and P. ROKKANEN, *Clin. Orthop. Rel. Res.* **268** (1991) 260.
23. P. A. MÄKELÄ, M. RUUSKANEN, N. ASHAMMAKHI, M. KALLIOINEN, T. POHJONEN, W. SERLO, P. TÖRMÄLÄ and T. WARIS, *Ann. Chir. Gynaecol.* **88** (1999) 318.
24. H. NIIRANEN and P. TÖRMÄLÄ, *J. Mater. Sci. Mater. Med.* **10** (1999) 707.
25. E. K. PARTIO, E. HIRVENSALO, O. BÖSTMAN and P. ROKKANEN, *Ann. Chir. Gynaecol.* **85** (1996) 67.
26. H. H. PELTONIEMI, R. M. TULAMO, T. TOIVONEN, D. HALLIKAINEN, P. TÖRMÄLÄ and T. WARIS, *J. Neurosur.* **90** (1999) 910.
27. P. ROKKANEN, *Annales chirurgiae et gynaecologiae* **80** (1991) 243.
28. P. U. ROKKANEN, O. M. BÖSTMAN, E. HIRVENSALO, E. A. MAKELA, E. K. PARTIO, H. PATIALA, S. VAINIONPÄÄ, K. VIHTONEN and P. TÖRMÄLÄ, *Biomater* **21** (2000) 2607.
29. A. SAIKKU-BACKSTROM, R. M. TULAMO, T. POHJONEN, P. TÖRMÄLÄ, J. E. RAIHA and P. ROKKANEN, *J. Mater. Sci. Mater. Med.* **10** (1999) 1.
30. I. SINISAARI, H. PÄTIÄLÄ, O. BÖSTMAN, E. A. MÄKELÄ, E. HIRVENSALO, E. K. PARTIO, P. TÖRMÄLÄ and P. ROKKANEN, *Acta Orthop. Scand.* **67** (1996) 16.
31. P. TÖRMÄLÄ, J. VASENIUS, S. VAINIONPÄÄ, J. LAIHO, T. POHJONEN and P. ROKKANEN, *J. Biomed. Mater. Res.* **25** (1991) 1.
32. P. TÖRMÄLÄ, *Clin. Mater.* **10** (1992) 29.
33. P. TÖRMÄLÄ, J. VASENIUS, S. VAINIONPÄÄ, J. LAIHO, T. POHJONEN and P. ROKKANEN, *J. Biomed. Mater. Res.* **25** (1991) 1.
34. P. TUOMPO, E. PARTIO and P. ROKKANEN, *Ann. Chir. Gynaecol.* **88** (1999) 66.
35. J. VASENIUS, S. VAINIONPÄÄ, K. VIHTONEN, M. MERO, A. MAKELA, P. TÖRMÄLÄ and P. ROKKANEN, *J. Biomed. Mater. Res.* **24** (1990) 1615.
36. D. D. WRIGHT, E. P. LAUTENSCHLAGER and J. L. GILBERT, *J. Biomed. Mater. Res.* **43** (1998) 153.
37. D. D. WRIGHT, E. P. LAUTENSCHLAGER and J. L. GILBERT, *ibid.* **36** (1997) 441.
38. J. L. GILBERT, D. S. NEY and E. P. LAUTENSCHLAGER, *Biomater* (1995) 1043.
39. D. D. WRIGHT, E. P. LAUTENSCHLAGER and J. L. GILBERT, *J. Mater. Sci. Mater. Med.* **10** (1999) 503.
40. W. J. PEERS, D. D. WRIGHT and I. MISKIOGLU, *Wear* (*submitted July 2003*) .
41. R. A. LATOUR, JR. and J. BLACK, *J. Biomed. Mater. Res.* **27** (1993) 1281.
42. D. D. WRIGHT, E. P. LAUTENSCHLAGER and J. L. GILBERT, *J. Appl. Polym. Sci.* **91** (2004) 4047.
43. D. D. WRIGHT, E. P. LAUTENSCHLAGER and J. L. GILBERT, *J. Biomed. Mater. Res.* **63** (2002) 152.
44. Standard test methods for flexural properties of unreinforced and reinforced plastics and electrical insulating materials [Metric], ASTM Specification D790M-86, ASTM Standards (ASTM, Philadelphia, PA, USA, 1990).
45. A. L. KING, *J. Appl. Phys.* **18** (1947) 595.
46. L. H. SPERLING, "Introduction to Physical Polymer Science" (John Wiley and Sons, Inc., New York, 1992).
47. Y. WANG and M. A. WINNIK, *Macromolecules* **26** (1993) 3147.
48. Y. LIU, G. REITER, K. KUNZ and M. STAMM, *ibid.* **26** (1993) 2134.

Received 25 February 2004
and accepted 11 March 2005